



Injectable polymeric nanoparticle hydrogel system for long-term anti-inflammatory effect to treat osteoarthritis

Bo-Bae Seo^a, Youngjoong Kwon^a, Jun Kim^{a,b}, Ki Hyun Hong^a, Sung-Eun Kim^c, Hae-Ryong Song^c, Young-Min Kim^{a,b,**}, Soo-Chang Song^{a,b,*}

^a Center for Biomaterials, Korea Institute of Science & Technology, Seoul, 02792, South Korea

^b Division of Bio-Medical Science and Technology, KIST School, Korea University of Science and Technology, Seoul, 02792, South Korea

^c Department of Orthopedic Surgery and Rare Diseases Institute, Korea University Medical College Guro Hospital, Seoul, 08308, South Korea

ARTICLE INFO

Keywords:

Thermosensitive hydrogel
Triamcinolone acetonide
Polymer nanoparticle
Osteoarthritis
Sustained release

ABSTRACT

Treatment of osteoarthritis (OA) by administration of corticosteroids is a commonly used method in clinics using anti-inflammatory medicine. Oral administration or intra-articular injection of corticosteroids can reduce the pain and progress of cartilage degeneration, but they are usually insufficient to show local and long-term anti-inflammatory effects because of their fast clearance in the body. In this study, we suggest an injectable anti-OA drug depot system for sustained drug release that provides long-term effective therapeutic advantages. Amphiphilic poly(organophosphazene), which has temperature-dependent nanoparticle forming and sol-gel transition behaviors when dissolved in aqueous solution, was synthesized for triamcinolone acetonide (TCA) delivery. Because hydrophobic parts of the polymer can interact with hydrophobic parts of the TCA, the TCA was encapsulated into the self-assembled polymeric nanoparticles. The TCA-encapsulated polymeric nanoparticles (TePNs) were well dispersed in an aqueous solution below room temperature so that they can be easily injected as a sol state into an intra-articular region. However, the TePNs solution transforms immediately to a viscose 3D hydrogel like a synovial fluid in the intra-articular region via the conducted body temperature. An *in vitro* TCA release study showed sustained TCA release for six weeks. One-time injection of the TePN hydrogel system in an early stage of OA-induced rat model showed a great inhibition effect against further OA progression. The OA-induced knees completely recovered as a healthy cartilage without any abnormal symptoms.

1. Introduction

Osteoarthritis (OA) is the most common type of degenerative joint disease [1]. Degeneration and inflammation of the joint lead to chronic pain, stiffness, and a progressive loss of articular cartilage that cannot be regenerated afterward [1,2]. Even though the degenerated joint could be replaced with artificial prostheses for the end-stage of osteoarthritis, the artificial prostheses are also limited and may invite additional surgery for artificial-joint replacement [3,4]. Other therapeutic strategies such as intra-articular (IA) administration of autologous chondrocytes [5], platelet-rich plasma [6], or visco-supplementation like hyaluronic acid (HA) onto the eroded cartilage could be other options for regeneration of damaged articular cartilage [7,8]. However, the resultant anti-OA effects of these methods are frequently unsatisfactory because

their target-specific action and remaining periods are poor after IA administration [9–11].

As a medicinal therapy, oral administration of analgesics, nonsteroidal anti-inflammatory drugs (NSAIDs), specific cyclooxygenase (COX)-2 inhibitors, and opioids would be the first option [1,9]. However, this treatment method is restrictively effective for the care of symptomatic pain and rarely effective for the topical treatment of inflammation [12]. Moreover, NSAIDs, COX-2 inhibitors, and opioids frequently lead to significant side effects on the gastrointestinal (GI) system, heart, and brain [12,13]. Therefore, these oral drugs should be prescribed carefully for older people who have underlying diseases with the GI system, heart, and brain. To increase the bioavailability of the administered medicine at the target site and reduce the possible systemic side effects, direct IA administration of corticosteroids such as

Peer review under responsibility of KeAi Communications Co., Ltd.

* Corresponding author. Center for Biomaterials, Korea Institute of Science & Technology, Seoul, 02792, South Korea.

** Corresponding author. Center for Biomaterials, Korea Institute of Science & Technology, Seoul, 02792, South Korea.

E-mail address: scsong@kist.re.kr (S.-C. Song).

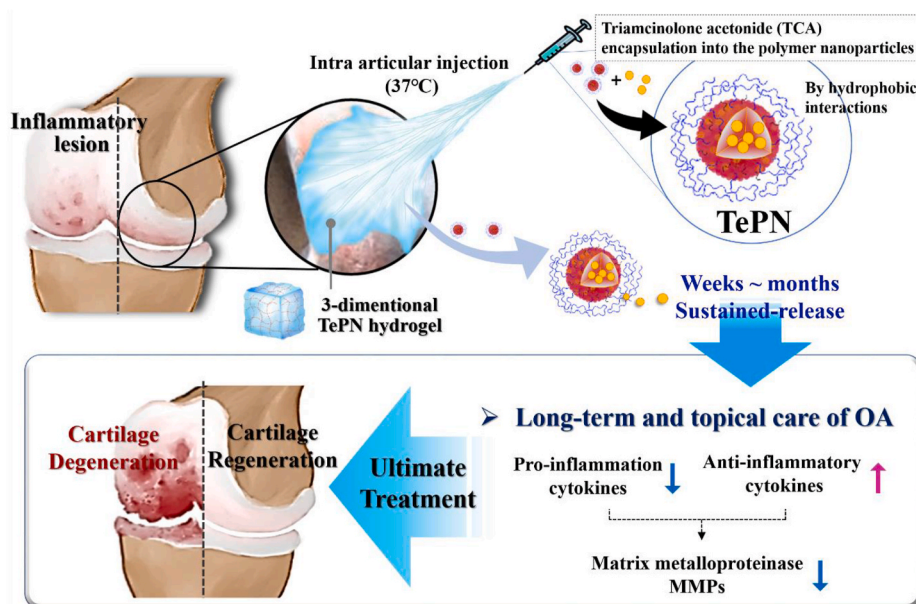
<https://doi.org/10.1016/j.bioactmat.2021.05.028>

Received 22 March 2021; Received in revised form 12 May 2021; Accepted 12 May 2021

Available online 7 July 2021

2452-199X/© 2021 The Authors. Publishing services by Elsevier B.V. on behalf of KeAi Communications Co. Ltd. This is an open access article under the CC

BY-NC-ND license (<http://creativecommons.org/licenses/by-nc-nd/4.0/>).



Scheme 1. Schematic diagram of one-time injection of the TePN hydrogel system for long-term osteoarthritis treatment.

methotrexate, diclofenac, and triamcinolone acetate (TCA) are also available [14–16]. However, their fast clearance has been reported; the half-lives of methotrexate, diclofenac, and TCA are from 0.56 to 2.9, 5.2, and 1.47 h, respectively [17–20]. These short retention times are not sufficient to diminish the persisting inflammatory responses.

For this reason, the development of a new strategy for the ultimate treatment of OA and timely prevention in the early stages has gained increased attention. Potential new OA treatment methods with long-term active anti-OA drug delivery systems have been attempted in various forms, such as liposomes [17,21], nanoparticle [22,23], microparticles [24,25], and hydrogels [26–28]. Liposomes and nanoparticle and macroparticle systems showed considerably extended periods of sustained anti-OA drug release over weeks to months [29,30]. However, these systems are unsuitable for exact localization at the target site and have unfavorable drug loading process with low release efficiency [31]. On the other hand, hydrogel-based drug delivery systems can provide localized drug depot advantages which can extend the drug release period and offer a physically supportable 3-dimensional (3D) space like a synovial region. These properties may further reduce damage to the synovial joint by reducing the physical friction in inflammatory arthritis. Moreover, a thermoresponsive sol-gel transformation ability can provide noninvasive administration advantages [32]. However, there are reported limitations of the hydrogel-based anti-OA drug delivery systems—they showed drug release characteristics only up to few days [20, 33].

A hybrid system of nanoscaled drug delivery and 3D hydrogel formation could fulfill the requirements of a powerful tool for successful OA treatment. For this purpose, a poly(organophosphazenes), which has substituted hydrophobic and hydrophilic side chains, could be a good candidate as an injectable *in situ* hydrogel-forming, and biodegradable drug delivery carrier with favorable drug loading process and long-term drug release characteristics [34–36]. In an aqueous solution, the polymer exists in the form of unfolded chains or nanosized spherical particles according to changes in hydrophobicity with temperature alterations [37,38]. Based on these characteristics, various drugs with hydrophobic parts can be encapsulated into polymeric nanoparticles (PNs) by participating in the self-assembly process of PNs. In addition, the polymeric nanoparticles could form the 3D hydrogel networks above a certain concentration [39,40].

In this study, localized and sustained TCA delivery using the poly(organophosphazenes) based PN hydrogel system was studied in an OA-

induced rat model. TCA was chosen as a model drug of NSAIDs which is required to deliver because of its limitations such as adverse effect and fast clearance [18]. As the main force of the PN self-assembly is a hydrophobic interactions between hydrophobic side chains, water-insoluble TCA could easily be loaded into the hydrophobic core of the PN during the PN self-assembly process and formed the TCA encapsulated PN(TePN) particles. TePN solution turned into 3D hydrogel after intra-articular injection and the formed 3D TePN hydrogel released TePNs for months. Finally, long-term release of TCA treats OA through inhibited matrix proteinase (MMP) expressions only within the cartilages via decreased pro-inflammatory cytokine expressions and increased anti-inflammatory cytokine expressions. Effective prevention and long-term anti-OA treatment with fewer side effects were observed in *in vitro* and *in vivo* OA model (Scheme 1).

2. Materials and methods

2.1. Materials

Hexachlorocyclotriphosphazene was purchased from Sigma-Aldrich (USA) and purified by sublimation at 55 °C under vacuum (about 0.1 mmHg). Poly(dichlorophosphazene) was prepared as described previously [42]. Methoxy poly(ethylene glycol) with molecular weight of 750 Da (Sigma-Aldrich, USA) was substituted to α -amino- ω -methoxy poly(ethylene glycol) (AMPEG) to substitute to the poly(organophosphazene) backbone as described in our previous work. The L -Isoleucine ethyl ester hydrochloride (IleOEt•HCl)(A&Z food additives, HangZhou, china, aminoethanol (Sigma-Aldrich, USA), glutaric anhydride (Alfa Aesar, USA), and 4-(dimethylamino) pyridine (DMAP)(Alfa Aesar, USA) were purchased. Tetrahydrofuran (THF) and trimethylamine (TEA) were dried by reflux over sodium metal and barium oxide respectively under dry nitrogen. Triamcinolone acetonide (TCA) was purchased from TCI (Japan). All other reagents were purchased from commercial suppliers.

2.2. Synthesis of poly(organophosphazenes)

All reactions were carried out under dry nitrogen atmosphere by using standard Schlenk-line techniques.

2.2.1. Synthesis of precursor polymer (PP, aminoethanol poly(organophosphazene))

Precursor polymer (PP) was prepared as elucidated below. First, IleOEt•HCl (10.8 g, 55.22 mmol) was suspended in dry THF (200 mL) and the reaction flask was cooled down. Second, poly(dichlorophosphazene) (10.00 g, 8.63 mmol) was dissolved in dry THF (200 mL), then slowly added to the prepared reaction flask containing IleOEt•HCl (23.64 g, 12.08 mmol) which dissolved in dry THA and TEA. The reaction mixture was stirred at dry ice bath for 12 h and then at 45 °C for 24 h. Third, AEtOH (1.42 g, 2.33 mmol) and AMPEG750 (13.59 g, 18.12 mmol) were dissolved in dry THF, and added to the reaction mixture. The reaction mixture was stirred at room temperature for 24 h and at 45 °C for another 24 h. The reaction mixture was filtered and poured into *n*-hexane to obtain a precipitate, which was then reprecipitated twice in the same solvent system. The polymer product was further purified by dialysis with a dialysis membrane (Spectra/Por, MWCO: 10–12 kDa) against methanol for 4 days at room temperature and against distilled water for 4 days at 4 °C. The dialyzed solution was freeze-dried to obtain PP. Yield: 73.7%. ¹H NMR(CDCl₃), δ(ppm): 0.8–1.0 (s, 6H), 1.1–1.3 (b, 3H), 1.3–1.6 (b, 2H), 1.6–1.9 (b, 1H), 2.8–3.3 (b, 2H), 3.4–3.8 (b, 73H), 3.9 (s, 1H), 4.0–4.3 (b, 3H).

2.2.2. Synthesis of carboxylic acid termini-functionalized poly(organophosphazene)(CP)

Carboxylic acid termini-functionalized poly(organophosphazene) (CP) was synthesized. In order to substitute the hydroxyl termini to carboxylic acid termini, glutaric anhydride (2.85 g, 24.99 mmol) and 4-(dimethylamino)pyridine (DMAP) (3.06 g, 24.99 mmol) were added to the reaction flask containing PP (10 g, 12.25 mmol) which was dissolved in dried THF. The reaction mixture was stirred at room temperature for 12 h, and then heated up to 40–45 °C for another 24 h. The final product, CP, was dialyzed with a dialysis membrane against methanol for 3 days at room temperature and against water for 3 days at 4 °C. The purified CP was gained via freeze drying. The newly appeared peak at 2.1–2.32 ppm (b, 4H, CH₂) represents the generated glutaric acid termini that does not exist in the CP ¹H NMR. Yield: 96%. ¹H NMR(CDCl₃), δ(ppm): ¹H NMR (300 MHz, CDCl₃, δ), d (ppm): 0.8–1.0 (s, 6H, CH₃), 1.1–1.3 (b, 3H, CH₃), 1.3–1.6 (b, 2H, CH₂), 1.6–1.9 (b, 1H, CH), 2.1–2.32 (b, 4H, CH₂), 2.8–3.3 (b, 2H, CH₂), 3.4–3.8 (b, 62H, CH₂), 3.9 (s, 1H, CH), 4.0–4.3 (b, 3H, CH₃).

2.3. Characterization of the CP

Structures of the synthesized CP were estimated by measuring ¹H NMR (Varian Gem-ini-300 spectrometer operating at 300 MHz in the Fourier transform mode with CDCl₃). Surface charge of the CP in aqueous solution was measured by Zetasizer Nano ZS (Malvern Instruments Ltd., Malvern, UK). The molecular weight (MW) of CP was calculated by a gel permeation chromatography system (Tosoh, EcoSEC HLC-8320 GPC) with a refractive index detector and two Styragel columns (TSKgel SupermultiporeHZ-M and TSKgel SuperHZ-2500) connected in line at a flow rate of 0.35 mL/min at 25 °C. THF containing 0.1 wt % of tetrabutylammonium bromide was used as a mobile phase. Polystyrenes (MW: 162; 580; 1920; 3090; 9590; 27,810; 70,500; 133,500; 290,300; 729,500; 1,074,000; 2,703,000) were used as standards.

2.4. Biocompatibility study

2.4.1. Cytotoxicity study of the CP

Cytotoxicity test of the CP was performed with mouse fibroblast cell lines (NIH3T3). Cells were seeded in a 96-well plate (SPL, Korea) with a density of 2×10^4 /well, and the cells were attached overnight in Dulbecco's modified Eagle's medium (DMEM) supplemented with 10% fetal bovine serum and 1% penicillin/streptomycin in humidified atmosphere of 5% CO₂ at 37 °C. The culture media was changed after 24 h with a

fresh DMEM, and various concentrations of the CP were treated (0 mg/mL to 10 mg/mL in DMEM, *n* = 6). After 24hr/48hr/72hr, the MTT solution (3-(4,5-dimethylthiazole-2-yl)-2,5 diphenyltetrazolium bromide) was treated and incubated for 3 h after suction of medium. The precipitates were dissolved in 100 μL of DMSO and the absorbance of the resulting purple solution was determined at excitation wavelength of 570 nm, using Spectra MAX 340 (BIO-RAD, Hercules, CA). The cell viability (%) was calculated from [ab]test/[ab]control × 100%.

2.4.2. Mutagenicity study of the CP

The mutagenicity of the CP was assessed with several auxotrophic strains of bacterium salmonella typhimurium. The amount of revertant colonies generation were evaluated to determine the mutagenicity (Ames test). For examination of T98 and T100 were performed with sterilized liquid medium (2.5% Oxoid Nutrient Broth No. 2). After 10 h of incubation inside shaking bath (37 °C, 200 rpm) 0.1 mL of cultured bacteria was mixed with 2 mL of top agar, 0.1 mL of CP solution, and S9 fraction. This mixture was then carefully poured onto previously prepared Petri dish which is containing 20 mL of minimal glucose agar plate and incubated until it solidified. After 48 h of incubation at 37 °C, the number of colonies was calculated. Phosphate buffered saline (PBS) was used as a negative control and 2-nitrofluorene, benzo(a)pyrene, and sodium azide were used as positive controls which are specific to each bacterium T98 and T100. All the negative and positive controls were conducted in a same manner. Minimal glucose agar plate was prepared by using Bacto agar (Difco), Vogel-Bonner medium E, and 2% glucose.

2.5. Preparation of self-assembled polymeric nanoparticles(PNs) and TCA-encapsulated polymer nanoparticle (TePN)

The synthesized CP were dissolved in PBS solution at 4 °C with magnetic stirrer (12 wt% CP solution was prepared, the ten times diluted). The prepared CP solution was observed by dynamic light scattering (DLS) with Zetasizer Nano ZS (Malvern Instruments Ltd., Malvern, UK) and by transmission electron microscopy (TEM, CM30 electron microscope, Philips, CA). The observed sizes and shapes of the self-assembled PNs were confirmed. The TCA-encapsulated polymer nanoparticles (TePN) were prepared with three different concentrations of TCA (0.3, 1.0 and 1.5 mg/mL). TCA were added to the PNs solution directly, and gently mixed. The mixed solution was incubated for 30 min in room temperature to induce TCA encapsulation. The characteristics of TePN were verified with DLS and TEM.

2.6. Thermosensitive sol-gel transition behaviors of the TePN solution

The viscosity of the aqueous PN solution (12 wt%) was measured by a Brookfield RVDV-III + visco-meter between 5 and 75 °C under a fixed shear rate of 0.1 s⁻¹. The measurements were processed with a set spindle speed of 0.2 rpm and with a heating rate of 0.33 °C/min. The measurement of rheology (MSC 102, Anton Paar, DE) was performed with the PN solution (12 wt% of PN in PBS) and the TePN solutions (0.3, 1.0, and 1.5 mg/mL of TCA was added to the prepared 12 wt% of PN solution). The measurement of storage modulus (G') and loss modulus (G'') were conducted with a gap length of 0.3 mm at an oscillating frequency of 1 Hz, 5% of the oscillating strain, and temperature in 4 °C and 60 °C.

2.7. In vivo degradation study of the TePN hydrogel

TePN solution (1.5 mg/mL of TCA, 200 μL) was injected to backs of mouse (Balb/c nude mice, 6 weeks, male, from Orient Bio, Korea) subcutaneously using a 31-gauge needle. Locally generated TePN hydrogels were identified right after the injection. The remained TePN hydrogels were weighted every pre-determined day.

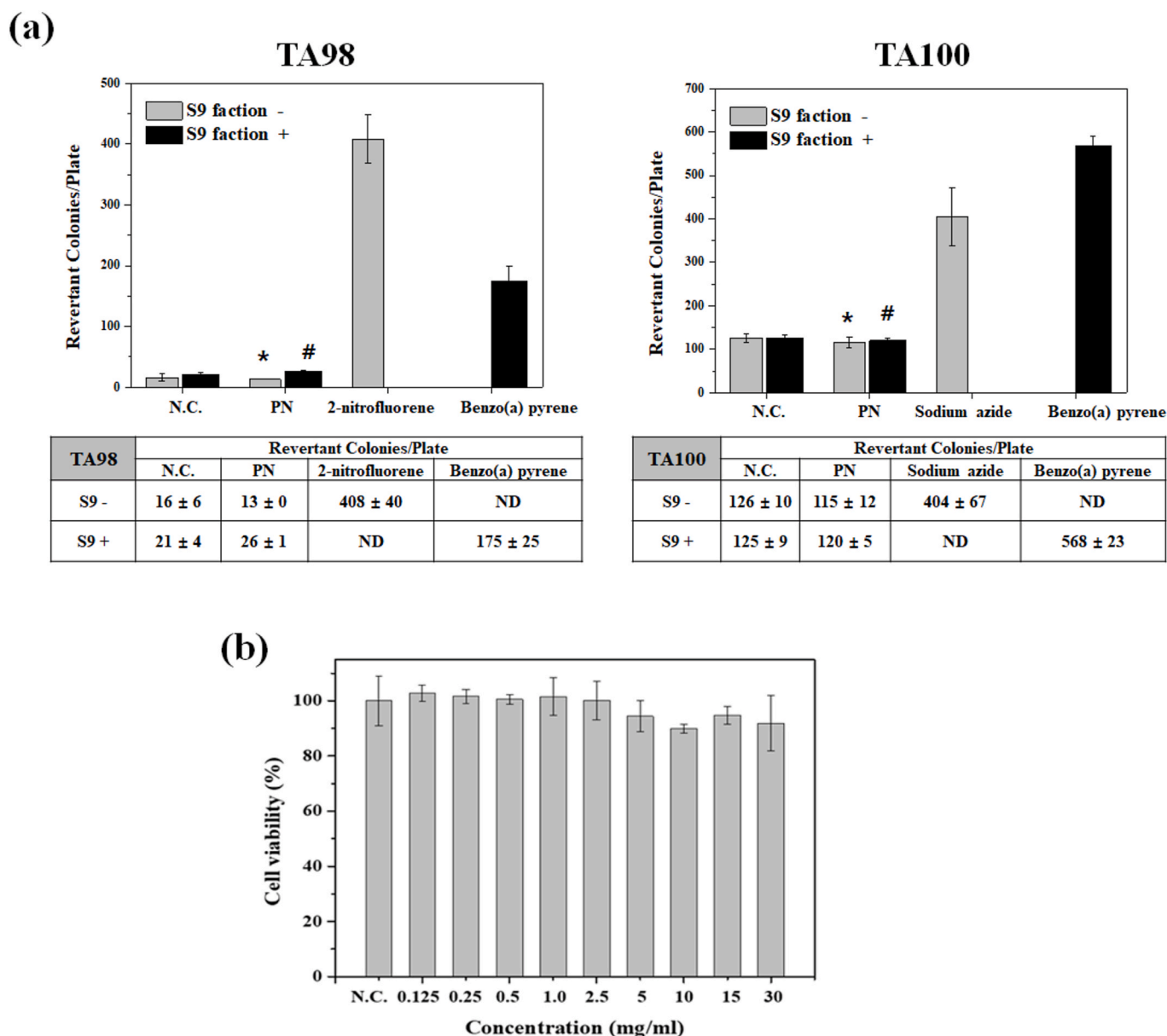


Fig. 1. Biocompatibility study of poly(organophosphazene) (a) Mutagenicity of PN was examined with negative control (N.C.) and positive controls. T98 and T100 are used as auxotrophic strains of bacterium *Salmonella typhimurium*. (*S9 was used as an activator for chemical substances that require metabolic activation to become mutagenic) (n = 3) (* indicates p < 0.01 vs 2-nitropyrene or Sodium azide, # indicates p < 0.01 vs Benzo(a) pyrene). (b) Cytotoxicity test of various concentrations of the PN (NIH 3T3 cell, n = 8).

2.8. In vitro release of TCA from TePN

TePN solution was prepared with 12 wt% PN solution with 0.3, 1.0, and 1.5 mg/mL of TCA, respectively. 0.3 mL of the prepared TePN solutions were loaded into tube, and hydrogel formation was identified by temperature increase to 37 °C. To the hydrogel, 6 mL of PBS solution gently added, and the tubes were incubated in water bath (KMC-12055W1, Vision, Korea) at 37 °C under mild shaking motion (50 rpm). The PBS solution was changed to fresh PBS solution at each time point. The amount of released TCA was measured by High Performance Liquid Chromatography (HPLC, Agilent) using water/acetonitrile(50/50, v/v %) as eluents with UV detection at 240 nm and calculated by established standard sample.

2.9. In vivo anti-OA effects of the TePN hydrogel system

2.9.1. Intra-articular injection of TePN in osteoarthritis(OA) bearing rats

Monosodium iodoacetate (MIA, Sigma-Aldrich, USA)(0.5 mg/50 µl) was injected to intra-articular region of Sprague Dawley(SD) rat(6 weeks, male from Orient Bio, Korea)(n = 6 for each group) to induce OA. After 1 week, OA induced rats were treated with 0.3 mL of TePN solutions by intra-articular injection. Non-treated MIA-induced OA rat model were used as control. Rats were sacrificed 8 weeks after the injection of TePN for further analysis.

2.9.2. Intra-articular structures and X-ray, micro-computed tomography (µ-CT) scanning

After sacrificing the rats at 8 weeks post injection, separated knee joints were cut down from the femur and tibia. The separated knee samples were scanned using X-ray (In-Vivo Series, DXS PRO,

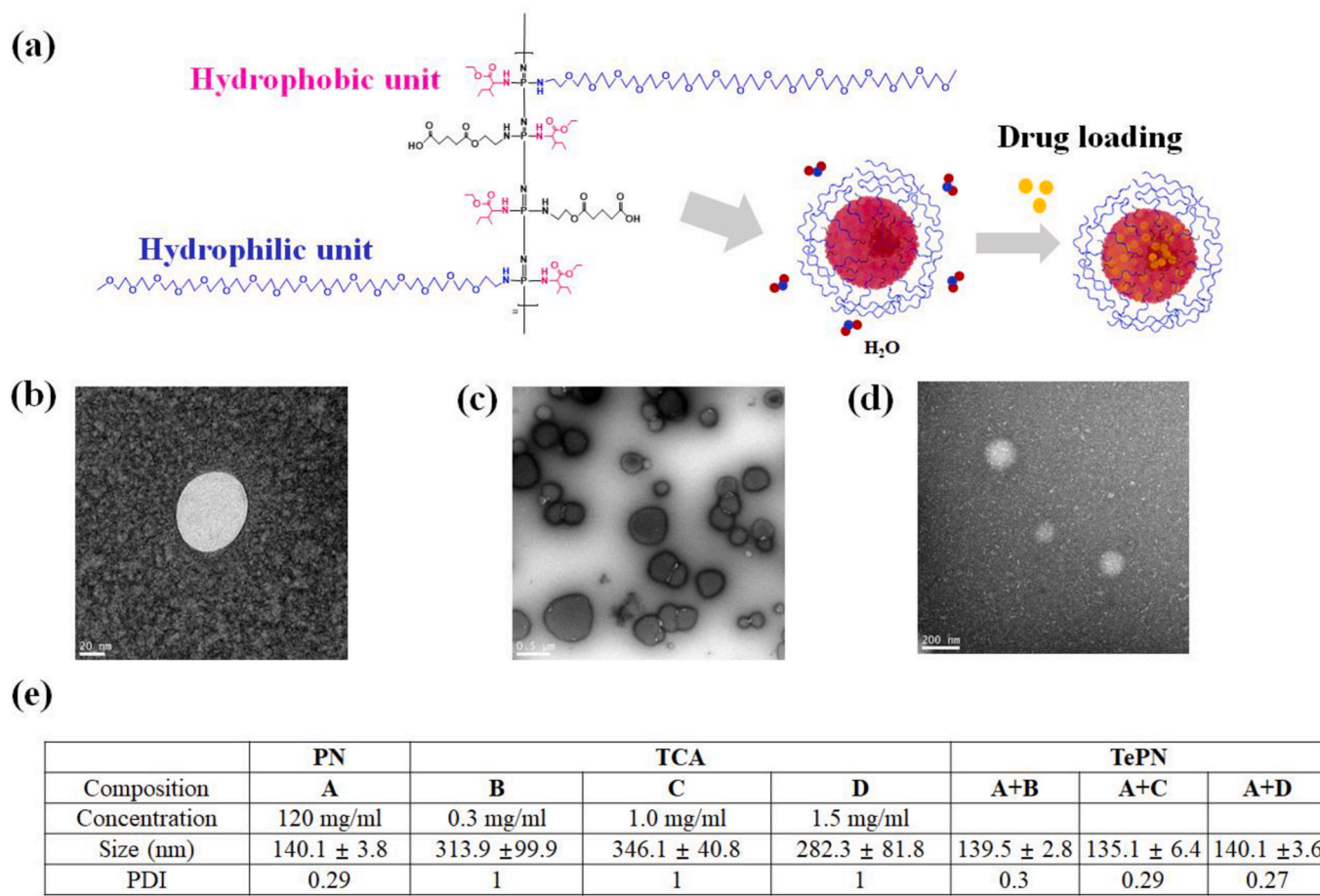


Fig. 2. Characterization of poly(organophosphazene) nanoparticles. (a) Structure of amphiphilic poly(organophosphazene) and their self-assembly behavior. TEM images of self-assembled PN (b), TCA aggregate (c) and TePN (d). (e) Hydrodynamic diameters of self-assembled PN, TCA aggregate, and TePN in PBS solution (n = 6).

Carestream, USA) and μ -CT (Aibira CT system, Carestream, USA). The distance of destroyed cartilages were measured using the μ -CT images and image J software.

2.9.3. Histological analysis

All collected tissues were embedded in paraffin and sectioned with a microtome (thickness 8 μ m). For histological evaluations, tissue sections were deparaffinized, rehydrated, and stained. The histological profiles of individual kness joint were observed by light microscope (Nikon; E400, Japan) after staining with hematoxylin and eosin (H&E) and safranin-O.

2.9.4. RNA isolation and real-time polymerase chain reaction

Blood samples were collected at each time point (after OA induction, 1-, 4-, and 8 weeks after the TePN hydrogel treatment). RNA was isolated using RNA blood kit (QIAamp, QIAGEN) according to the manufacturer's instruction. cDNA was synthesized using Accupower CycleScriptRT Pre Mix (dT20) (BIO-RAD) following the manufacturer's protocol. Real-time polymerase chain reaction (PCR) amplification and detection were performed using an ABI7300 Real-Time Thermal cycler (Applied Biosystems, Foster City, CA, USA). Gene expressions of pro-inflammatory cytokines such as metalloproteinase-3 (MMP-3), MMP-13, interleukin-6 (IL-6), and tumor necrosis factor- α (TNF- α) and anti-inflammatory cytokines such as IL-4, IL-10, and IL-13 were examined, respectively. The sequences of each gene markers are listed in (Table S1).

3. Results and discussion

3.1. Synthesis and characterization of poly(organophosphazene)

Poly (organophosphazene), which mainly contains a hydrophobic *L*-isoleucine ethyl ester (IleOEt) and hydrophilic α -amino- ω -methoxy poly (ethylene glycol) (AMPEG) on its side chains, was synthesized and used as a temperature-responsive and *in situ* gelling drug depot system. In addition, carboxylic acid termini were introduced to mimic the extracellular matrix of the natural cartilage, which is mainly composed of chondroitin sulfate and hyaluronic acid, and interact with several cytokines relevant to homeostasis and regeneration of cartilage (Fig. S1).

The molar ratios of the substituted side chains were calculated using NMR spectra. The concentration of IleOEt, AMPEG, and carboxylic acid was 70%, 10.5%, and 13.5% in the final polymer, respectively. The substituted rates of each composites of the polymer were evaluated by integrations of the specific peaks, 0.8–1.0 ppm for 6 protons of IleOEt/ 2.1–2.32 ppm for 4 protons of carboxylic acid/3.4–3.8 ppm for 62 protons of AMPEG in ¹H NMR data (Fig. S2). The electric charge of the final polymer was characterized by zeta potential measurement as -4.0 ± 1.6 , negative charge to mimic extracellular matrix of cartilage, and GPC analysis with polystyrene standards showed a molecular weight of 50,085 Da.

3.2. Biocompatibility study of poly(organophosphazene)

Biocompatibility is an indispensable factor for the development of new drug delivery carriers. The Ames test is commonly test to evaluate

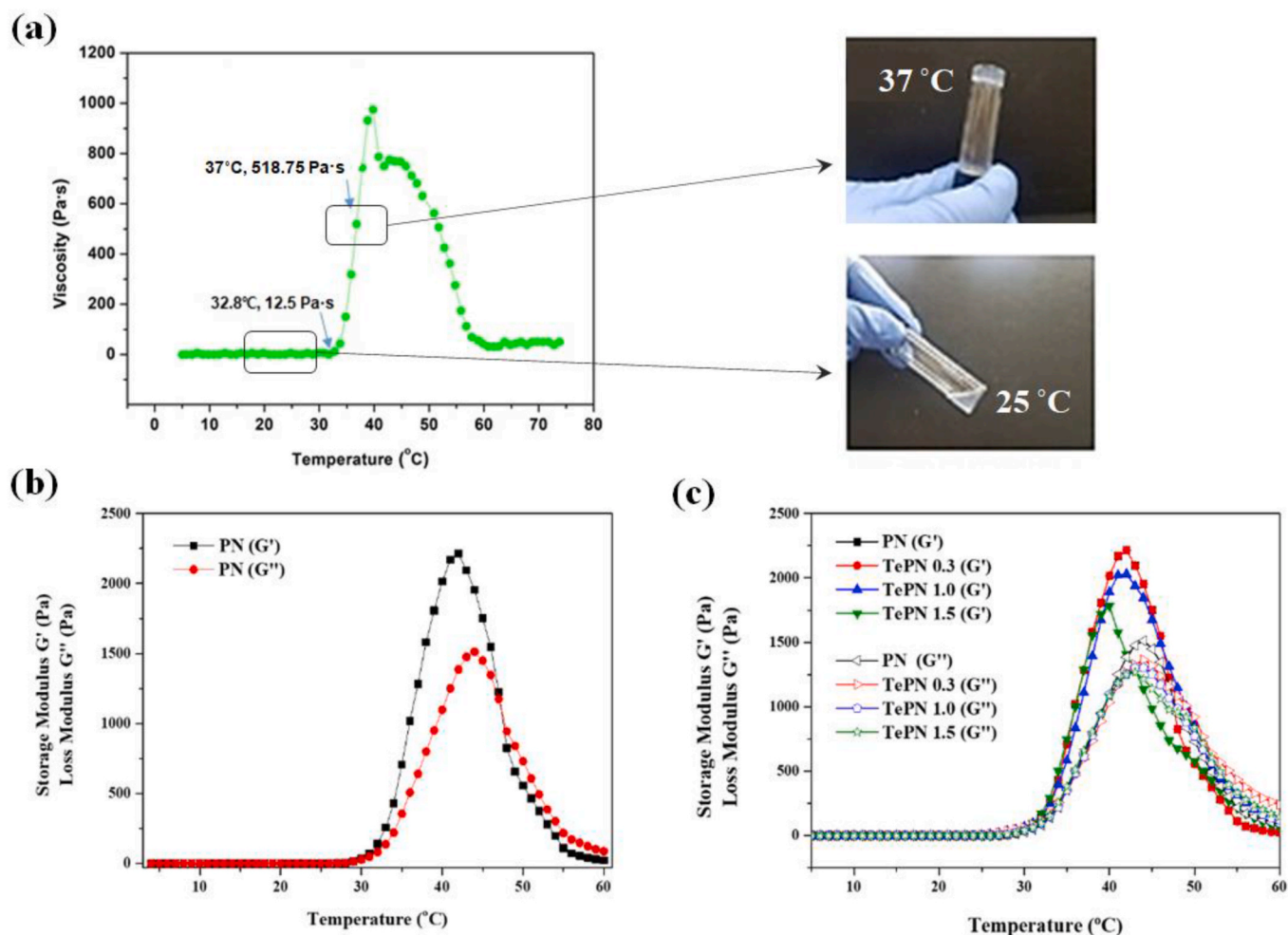


Fig. 3. Characterization of the TePN hydrogel system. (a) Temperature-dependent sol-gel transition and viscosity changes of PN solution (12 wt % in PBS solution). (b) Temperature-dependent changes on storage and loss modulus of 12 wt% PN solution. (c) Temperature-dependent changes on storage and loss modulus of TePN solutions.

the potential mutagenicity of testing chemicals, which is related to carcinogenic potential. For the mutagenicity test, *Salmonella typhimurium* TA98 or TA100 were treated with 200 μg of the polymer. The polymer-treated group showed approximately the same revertant colonies as the negative controls. (Fig. 1a). These no-cytotoxicity and mutagenic responses imply the safety of the synthesized polymer, and these results may support the possibility that the polymer could be used as a bioavailable material. Especially for anti-OA treatment, the TCA carrier requires highly biocompatible properties because the carrier should not promote the immune responses at the site of lesion. For this reason, the investigated biocompatibilities of the synthesized poly(organophosphazene) are appropriate as an anti-OA drug delivery carrier.

Cellular toxicity and mutagenicity tests are required to generate toxicity data for new drug or bioavailable materials. For these reasons, the toxicities of the synthesized poly(organophosphazene) were investigated by MTT assay and Ames test. The cytotoxicity of the polymer was treated with the NIH 3T3 cell line (from 0 mg/mL to 30 mg/mL concentration of polymer in media). Twenty-four hours after treatment, 90–95% cell viability was observed at every polymer concentration (Fig. 1b). Even after treatment of the polymer with same composition with the CP for 48, 72 h, there were no cytotoxic effects and it means the CP is a cytocompatible material. (Fig. S3).

3.3. Characterization of self-assembled PNs and TCA encapsulation

Side chains on the polymer were occupied with hydrophobic and hydrophilic moieties to have balanced amphiphilicity. The polymer exists as spherical nanoparticles in an aqueous environment to minimize the exposed area of the hydrophobic IleOEt units on the polymer against water molecules. Moreover, water-insoluble drugs such as TCA interact with the hydrophobic core parts of the PNs (Fig. 2a). The self-assembled PNs and TePNs were investigated by TEM and size distribution studies. The round-shaped PNs were identified by the TEM image (Fig. 2b), and their size was ~ 140 nm around 25 $^{\circ}\text{C}$ (120 mg/mL of PNs in phosphate buffered saline (PBS) solution) with an error range of ≤ 4 nm. TCA, a poor water-soluble drug, showed irregular nano- and microsized crystallin in PBS solution (1.5 mg/mL TCA in PBS) with a range from 232.9 to 3343 nm with an error range of ≥ 1450 nm in the DLS and TEM data (Fig. 2c and Fig. S4). However, the microsized TCA aggregates disappeared from the size distribution after mixing and incubation with the PN-dispersed PBS solution. Only ~ 140 nm sized particles were measured with an error range of ≤ 4 nm in the mixture solution of TCA and PN (120 mg/mL of PNs and 1.5 mg/mL of TCA in PBS solution) (Fig. 2d). This result supports the successful encapsulation of TCA onto the PN nanoparticles. The average sizes and poly dispersity index (PDI) values of these particles are summarized in Fig. 2e and Fig. S5. The size changes and significant decrease strongly support our prediction that TCA could be well encapsulated into the hydrophobic core of the PN by

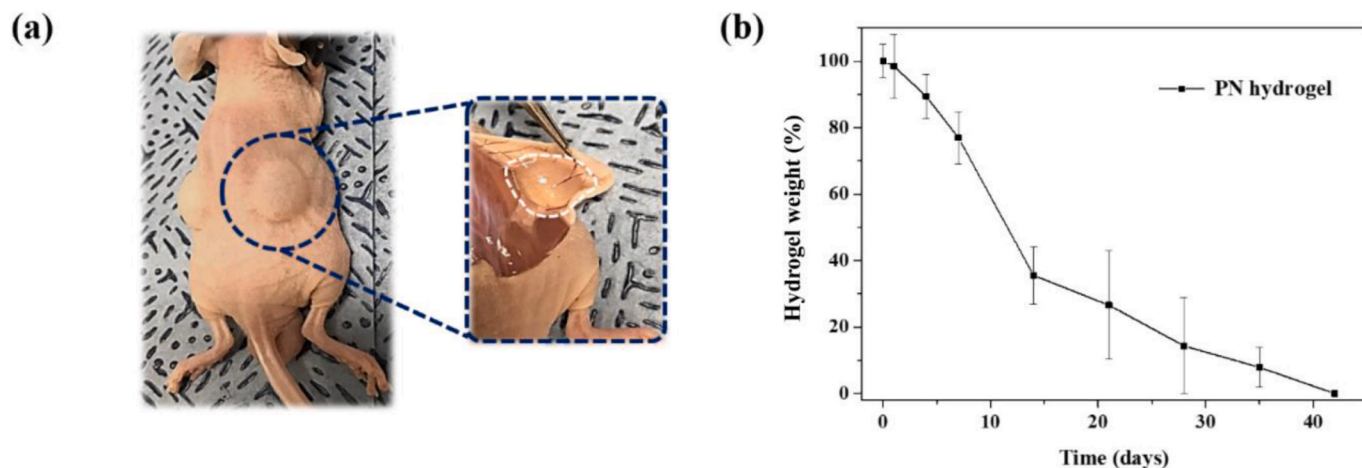


Fig. 4. Biodegradation study of PN hydrogel system. (a) Visualization of the injectability and hydrogel formation of TePN hydrogel system. (b) Time-dependent hydrogel degradation after injection of 12 wt% PN solution (n = 3).

its hydrophobic interactions.

3.4. Thermosensitive sol-gel transition behaviors of the TePN solution

Above a certain concentration of the PN in aqueous solution, there are clear viscosity and phase alternations according to temperature changes. These phase transitions are caused by the weakening hydrogen bonds between the hydrophilic PEG chains on the PN and water

molecules with increasing temperature, whereas the hydrophobic interactions among the PNs increased. In this study, 12 wt% of PN solution was prepared to have good injectability, sufficient viscosity, and maximum storage modulus to be in gel state at the body temperature. As shown in Fig. 3a, the PN solution showed a viscosity of 0 Pa s until 32 °C. The viscosity values continuously increased from 32 °C and showed 518.75 Pa s at 37 °C. Similarly, both storage and loss modulus values increased from 32 °C, and the storage modulus value (G') was greater

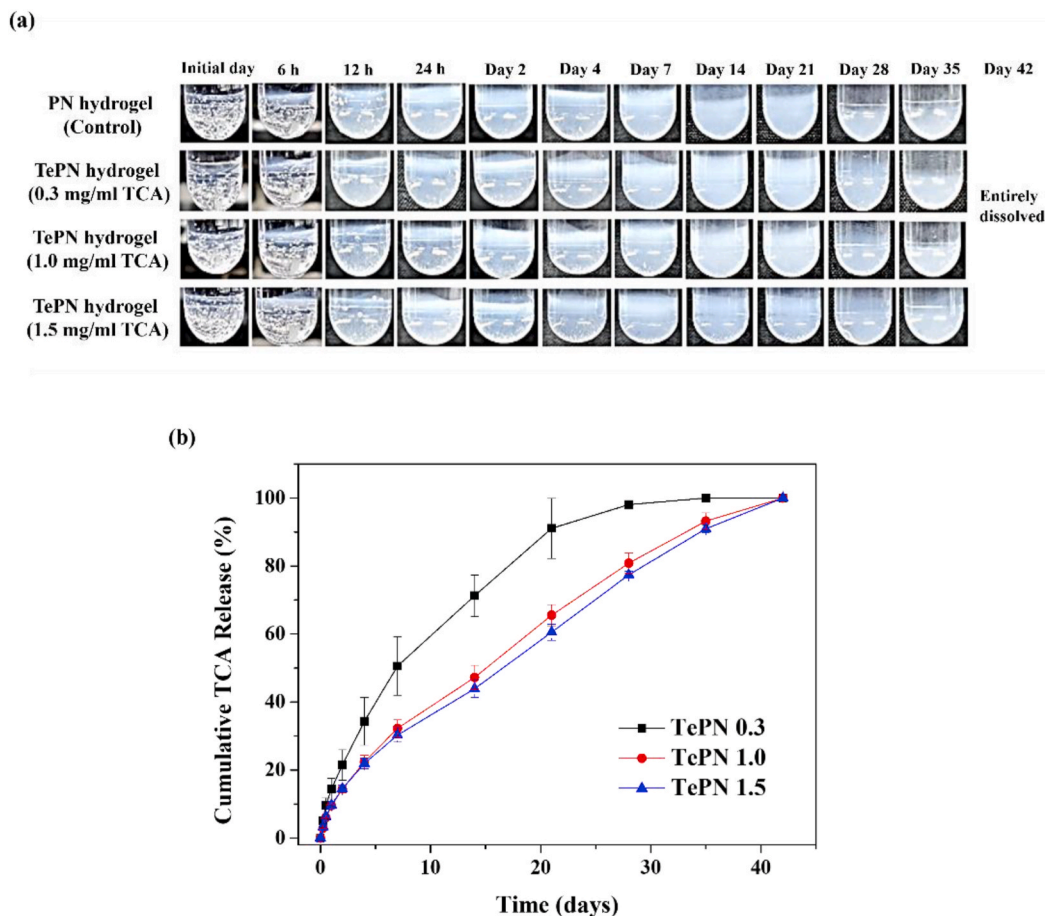


Fig. 5. Sustained release profile of TCA from TePN hydrogel system *in vitro*. (a) Time-dependent hydrogel state of TePN hydrogels. (b) Cumulative TCA release behaviors of the TePN hydrogels with each concentration of TCA.

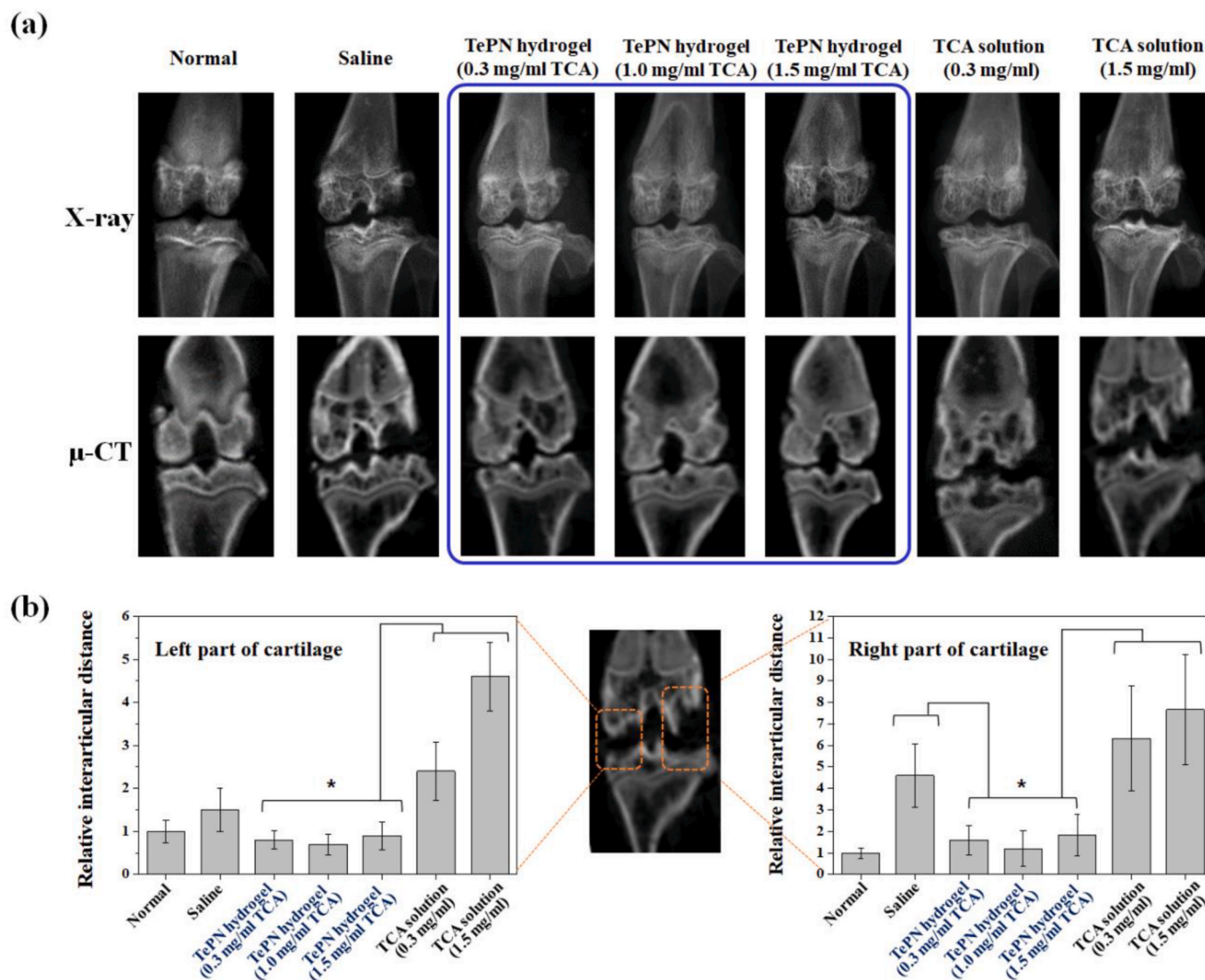


Fig. 6. *In vivo* anti-inflammatory efficiency of TePN after IA injection. (a) X-ray and (b) μ -CT images of each group taken at 8 weeks after the treatment. Distance of interarticular cartilage (DIC) in the left part (c) and right part (d) of the cartilage ($n = 5$, *: $p < 0.01$).

than that of the loss modulus value (G'') between 32 °C and 44 °C from the rheology study. At 37 °C, the G' and G'' values were 1284.3 and 765 pa, respectively, that indicating a gel state (Fig. 3b).

As shown in Fig. 3c, the sol-gel transition behaviors were monitored after TCA loading because the physical properties of the drug delivery hydrogel may considerably affect the drug release pattern or period. The storage and loss moduli of the TePN solutions were measured after TCA loading with three different doses. All the groups showed similar changes in the storage and loss modulus values according to the temperature changes. These results may demonstrate that the loaded TCA was encapsulated homogeneously inside the PN and rarely affected the sol-gel transition behaviors, and these properties facilitate predictability of the hydrogel's condition even with variable drug doses.

3.5. *In vivo* degradation of the TePN hydrogel

Because biodegradation is an essential requirement for a biomaterial and drug delivery carrier, the hydrogel degradation rates and common symptoms around tissues in which PN hydrogel was locally placed were monitored. The prepared PN solution was injected under the skin of a mouse with a 31-gauge needle. The formation of PN hydrogel was directly identified after the injection, and the remaining PN hydrogels

were weighed after a simple separation procedure from the skin at intended time points (Fig. 4a). The amounts of remaining PN hydrogels decreased with time until 42 d (Fig. 4b and Fig. S6). These biodegradation properties, mild conditions for the formation of PN hydrogel, and its long-term retention at the injected site indicates the suitability of developed PN hydrogel system for use as a long-term depot drug delivery carrier.

3.6. Sustained release profile of TCA from TePN *in vitro*

Steroidal anti-inflammatory drugs such as TCA have a short retention time after intra-articular administration and are cleared out quickly in our body. Therefore, the long-period anti-inflammation effect would be restrictive. The TePN hydrogel system could control the TCA release pattern and period by controlling the dissociation and degradation rates of the PN hydrogel because strongly interacting drugs tend to highly depend on the degradation properties of the material [36]. The TCA release behaviors were studied with freshly prepared TePN solution containing three different concentrations of TCA. After formation of the TePN hydrogel at 37 °C, each of the TePN hydrogels were soaked in a PBS buffer. In contrast to the PN group showing rapid swelling less than 1 day, most hydrogels with TCA showed swelling after 1 week because

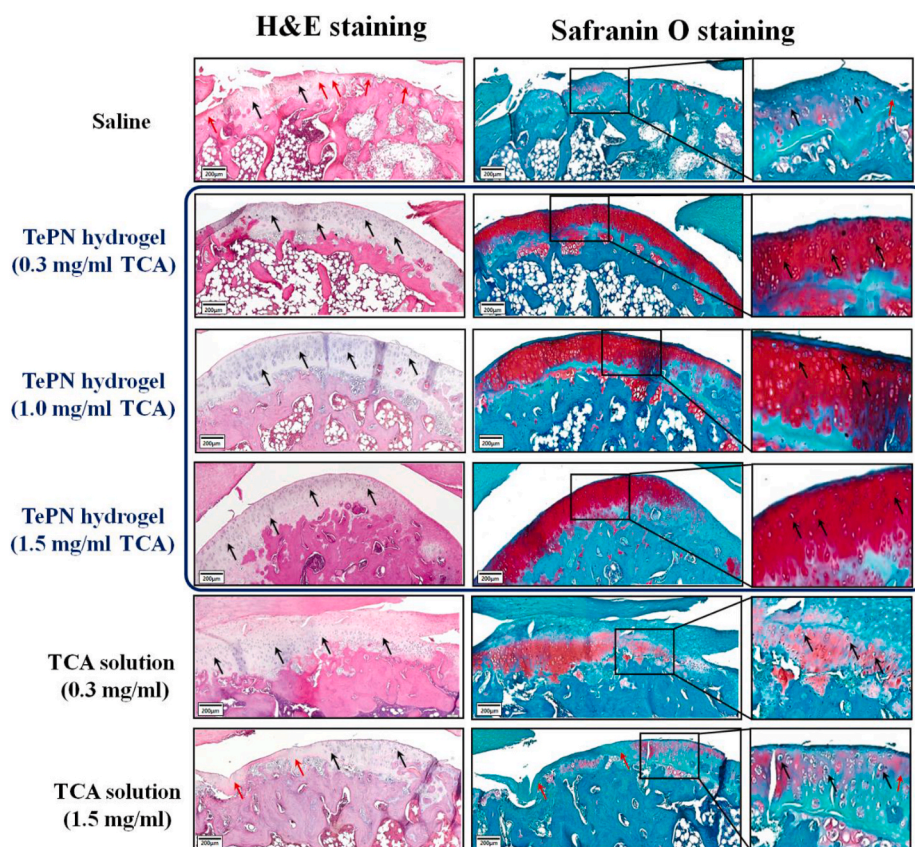


Figure 7. *In vivo* anti-inflammatory efficiency of TePN hydrogel systems. Histological staining of H&E (black arrow: tissues w chondrocytes/red arrow: tissues w/o chondrocytes) and safranin O (red; glycosaminoglycans, scale bar; 200 μ m) after 8 weeks from the treatment.

hydrophobic interactions between TCA and the hydrogels enhance stability of the polymer structure in aqueous solution (Fig. S7). And all the gels started mass losses after 4 weeks (Fig. 5a). It closely correlated with TCA release patterns from the hydrogels during 42 days (Fig. 5b). Inhibited initial burst of TCA was identified during the first 24 h in the three TePN hydrogel groups with TCA concentrations of 0.3, 1.0, and 1.5 mg/mL and the observed values read as 14.45%, 9.55%, and 9.72% compare to the total amount of loaded TCA, respectively. These results are in contrast with the half-life of naked TCA without a delivery carrier being only 1.27 h in the human body when administered directly. In each TePN hydrogel group, approximately half the amount of loaded TCA was released on days 7, 14, and 16 with values as 0.3, 1.0, and 1.5-mg/mL, respectively. The sustained-release process lasted until the entire degradation of the TePN hydrogels. Meanwhile, the TePN hydrogel group with the lowest TCA concentration showed a faster release pattern than the other two groups. The low TCA concentration possibly affects the loss of hydrophobic networks, rapid swelling, and fast dissolution. In the TePN hydrogel groups with 1.0 mg/mL and 1.5 mg/mL of TCA, the time-dependent TCA release pattern was quite linear. The degradation of the TePN hydrogel and the TCA release periods were almost similar. The suppressed initial burst release and continuous TCA release demonstrate that the TCA strongly interacts with the polymer and is well encapsulated by the PN.

3.7. Effects of long-term anti-inflammation and cartilage degeneration prevention by one-time injection of the TePN hydrogel in OA rat model

The effects of long-term anti-inflammation and inhibition of cartilage degeneration were verified by a one-time injection of the TePN hydrogel depot system. A rat model bearing monosodium iodoacetate (MIA)-induced OA was prepared for the treatment of the TePN hydrogel

system. The TePN injection was carried out 1 week after the generation of OA to mimic the early stage of OA. In addition to the TePN hydrogel groups, direct injection of the TCA solution and saline groups were added as controls. Each 300 μ l solutions of saline, TePN, and TCA were prepared freshly and injected to the injured sites of the rats.

Eight weeks after the treatment, the knee joints of sacrificed rats were dissected and it was found that only TePN-treated groups showed clear and rare inflammatory reactions comparing with the other groups (Fig. S8). X-ray and μ -CT images were also taken for morphological studies (Fig. 6a). The saline-treated group showed considerably progressed OA with serious cartilage deflection and destroyed cartilage bone. However, each TePN-treated group demonstrated well-maintained morphological characteristics, indicating that the inflammation in the early stage of OA was well suppressed by the sustain-released TCA. Moreover, every TePN hydrogel group showed significant improvement in anti-OA effects compared with the TCA-solution groups. The destroyed cartilage status in direct TCA-solution injection groups reflects its failure in long-term inflammation care and prevention of cartilage degeneration. The pathological status of the cartilages in the TCA solution groups was similar or worse than that in the saline treatment group. This is because the possible side effects of direct IA injection of TCA on chondrocyte toxicity, and the topical treatment with a high dose of TCA may inhibit fibroblast growth and collagen synthesis by decreasing hydroxyproline production, which leads to decreased structural stability of connective tissue around the knee [12]. For statistical evaluation, the distance of interarticular cartilage (DIC) was measured (Fig. 6b). Most of the DIC was similarly increased in the saline- and TCA-solution treated groups in both the left and right parts, but only a statistically significant difference was confirmed between the saline and the high TCA-solution (1.5 mg/mL) groups in the left parts of the cartilage. The severe destruction of cartilage may result from two

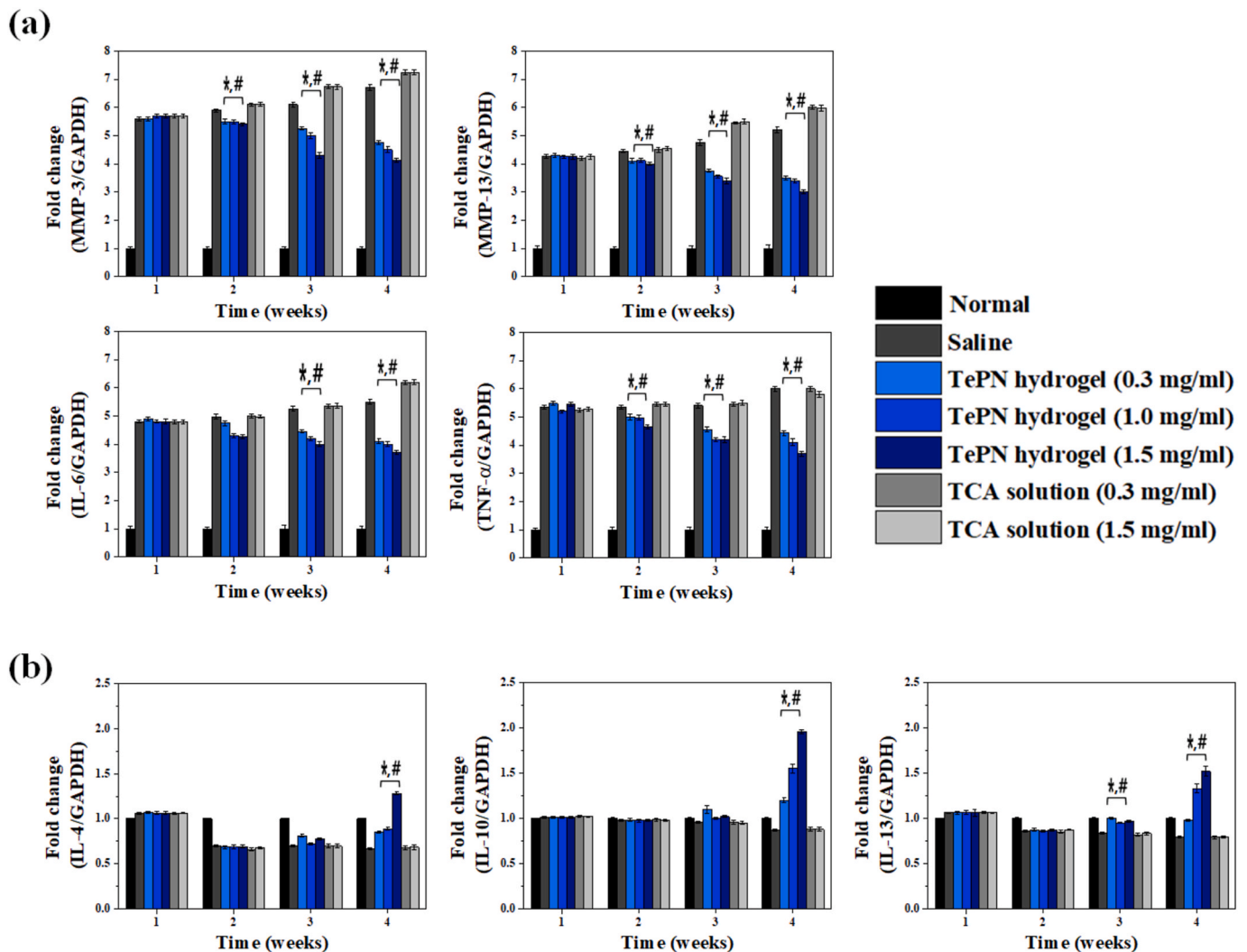


Fig. 8. Real-time PCR analysis. Blood samples were collected at each time point (1 week after the generation of MIA-induced OA, 1, 4 and 8 weeks after the treatment) to examine the gene expressions of pro-inflammatory cytokines such as MMP-3, MMP-13, IL-6, TNF- α (a) and anti-inflammatory cytokines such as IL-4, IL-10, and IL-13 (b) ($n = 6$): * $p < 0.01$ vs saline group, # $p < 0.01$ vs TCA solution treated groups).

reasons: 1) the possible toxicity of the direct TCA exposure in a short time with a high dose, and 2) inadequacy of the continuous anti-inflammation effect because of fast TCA clearance.

In addition, the contrasting results of well-prevented cartilage degeneration in the TePN hydrogel groups and the failure of OA treatment in direct TCA solution injection groups were demonstrated by histological staining methods (Fig. 7). Hematoxylin and eosin (H&E) and safranin O staining showed the morphological characteristics of each experimental group. The saline- and TCA-solution-treated groups showed thinning of the cartilage shape, losing the tissues with chondrocytes and disappearance of the characteristic red staining of glycosaminoglycans identified in healthy cartilage. These results indicate that the treatment of saline and TCA solution rarely influenced the progression of OA after the occurrence of the early stage. However, the TePN hydrogel groups showed morphological similarity with a normal cartilage, and the cellular characteristics of chondrocytes were well maintained. From this experiment, we can see that the sustained release of TCA via a one-time injection of the TePN hydrogel system could effectively prevent further inflammation and OA progression.

3.8. Effects of sustained TCA release using TePN hydrogel system on inhibition of pro-inflammatory genes and activation of anti-inflammatory genes

The alteration of inflammatory gene expression was evaluated during the experimental period. The expression levels of pro- and anti-inflammatory genes were evaluated from the corrected blood samples. A week after the generation of MIA-induced OA, gene expression levels of pro-inflammatory cytokines, MMP-3, MMP-13, IL-6, and TNF- α , increased 5.60, 4.25, 4.80, and 5.35 times higher than that of the normal group, respectively (Fig. 8a). After the injection of TePN or TCA solutions, contrasting gene expression patterns were observed in each experimental group at 1, 4, and 8 weeks after the treatment. The increased gene expression levels of pro-inflammatory cytokines decreased with time in the TePN hydrogel groups, although the TCA solution groups showed a continuous increase. Because the expression of pro-inflammatory cytokines and MMPs leads to cartilage degeneration, effective lowering of pro-inflammatory and MMPs cytokines may demonstrate the successful prevention of cartilage degeneration. After 8 weeks, the levels of MMP-3, MMP-13, IL-6, and TNF- α cytokine genes in the TePN hydrogel with the highest TCA concentration were identified with 1.62-, 1.67-, 1.49-, and 1.62-times decreased values as compared to that with the saline-treated group, respectively. In contrast, level of each

pro-inflammatory cytokine gene continuously increased over time in the TCA solution groups. Because directly administered TCA is cleared rapidly, the anti-inflammatory effects are insufficient to prevent the breakdown of the extracellular matrix and degradation of collagens in cartilage with one-time IA injection of TCA solutions.

The anti-inflammatory cytokine genes, such as IL-4, IL-10, and IL-13, were simultaneously monitored (Fig. 8b). These gene expressions are related to stimulation of immune cells such as macrophages and to certain T cells (Th2) on their survival, proliferation, and differentiation [43]. In addition, the expression levels of these cytokines could be a criterion for the inhibition of the synthesis of pro-inflammatory cytokines such as interferon-gamma, interleukins, and TNF- α [44]. One week after the generation of MIA-induced OA, the IL-4, IL-10, and IL-13 gene expression levels in all treatment groups were almost similar to the normal status. There were no significant differences among the treatment groups up to 4 weeks after the induction of inflammation. However, after 8 weeks, each gene expression level was significantly increased in the TePN hydrogel treatment groups. In addition, the increase margins of the gene expression expanded according to the concentration of the loaded TCA. After 8 weeks, IL-4, IL-10, and IL-13 gene expression levels in the TePN hydrogel with the highest TCA concentration were 1.91, 2.25, and 1.92 times higher than to that in the saline treated group, respectively. These results support the efficiency of sustained TCA release and their long-term anti-inflammatory effects via a one-time injection. There were no abnormal symptoms with respect to body weight (Fig. S9). The TCA unloaded PN hydrogel treatment showed no changes in the expression levels of pro- and anti-inflammatory genes, thereby indicating that the carrier PN hydrogel system showed no effects on systemic inflammatory responses.

4. Conclusion

A long-term and effective anti-OA treatment system was developed using poly(organophosphazene) nanoparticles that can encapsulate TCA and form a hydrogel after administration into the body. The proposed system aimed to overcome the rapid TCA efflux from the joint into systemic circulation after IA injection of TCA. The injectable TePN hydrogel system showed synergistic functions of physically supporting 3D hydrogel formation and sustained TCA release with a long-term anti-inflammatory effect. The TePN solution could be injected as a solution state around room temperature, and it transforms into hydrogel directly after IA injection due to the body temperature. Then, the encapsulated TCA is released slowly by loosening the TePN hydrogel networks and the degradation of the polymer. As a result, the release of TCA continued until the entire erosion and degradation of the TePN hydrogel. Released TCA could bind to glucocorticoid nuclear receptors, which are widely expressed in neurons and Schwann cells, the receptors undergo a conformational change and are translocated to the nucleus [45]. From these changes, gene transcription and induction of anti-inflammatory responses occur through the inhibition of pro-inflammatory responses cytokine release (e.g., TNF α and IL-1 β) [46]. Cartilage degradation was inhibited by the inactivation of MMPs via regressed pro-inflammatory cytokines. The proposed system has advantages comparing with other hydrogel based system such as 1) simple preparation with high drug loading efficiency (simple mixing between polymer solution and TCA), 2) Long-term delivery for a month only within injected site (no adverse effects), 3) Biocompatibility, 4) Cartilage environment mimics, and 5) Enhanced TCA efficacy (nanoparticle based enhanced delivery efficacy). Therefore, we believe that the proposed drug-encapsulating PN hydrogel system can be widely used as a platform delivery system for various drugs that have poor water-solubility and fast-clearance behavior after administration.

Data availability

All data obtained from this study are included in the article or

uploaded as supplementary information. The data that support the findings of this research are available from the corresponding authors upon reasonable request.

CRediT authorship contribution statement

Bo-Bae Seo: Investigation, Methodology, Formal analysis, Writing – review & editing. **Youngjoong Kwon:** Methodology, Formal analysis, Investigation. **Jun Kim:** Formal analysis, Investigation. **Ki Hyun Hong:** Formal analysis, Investigation. **Sung-Eun Kim:** Methodology, Formal analysis, Investigation. **Hae-Ryong Song:** Resources, Investigation, Formal analysis. **Young-Min Kim:** Conceptualization, Visualization, Writing – review & editing. **Soo-Chang Song:** Conceptualization, Visualization, Writing – review & editing.

Declaration of competing interest

The authors declare that they have no known competing financial interests or personal relationships that could have appeared to influence the work reported in this paper.

Acknowledgements

This research is financially supported by Korea Institute of Science and Technology (2E31121) and Korea National Research Foundation (2018M3A9H1024872).

Appendix A. Supplementary data

Supplementary data to this article can be found online at <https://doi.org/10.1016/j.bioactmat.2021.05.028>.

References

- [1] A.E. Nelson, Osteoarthritis year in review 2017: clinical, Osteoarthritis Cartilage 26 (3) (2018) 319–325, <https://doi.org/10.1016/j.joca.2017.11.014>.
- [2] N. Arden, M.C. Nevitt, Osteoarthritis: epidemiology, Best Pract. Res. Clin. Rheumatol. 20 (1) (2006) 3–25, <https://doi.org/10.1016/j.berh.2005.09.007>.
- [3] M. Khan, K. Osman, G. Green, F.S. Haddad, The epidemiology of failure in total knee arthroplasty: avoiding your next revision, Bone Joint Lett. J 98-B (1 Suppl A) (2016) 105–112, <https://doi.org/10.1302/0301-620X.98B1.36293>.
- [4] J.M. Quintana, I. Arostegui, A. Escobar, J. Azkarate, J.I. Goenaga, I. Lafuente, Prevalence of knee and hip osteoarthritis and the appropriateness of joint replacement in an older population, Arch. Intern. Med. 168 (14) (2008) 1576–1584, <https://doi.org/10.1001/archinte.168.14.1576>.
- [5] A. Mobasheri, G. Kalamegam, G. Musumeci, M.E. Batt, Chondrocyte and mesenchymal stem cell-based therapies for cartilage repair in osteoarthritis and related orthopaedic conditions, Maturitas 78 (3) (2014) 188–198, <https://doi.org/10.1016/j.maturitas.2014.04.017>.
- [6] L.G. Glynn, A. Mustafa, M. Casey, J. Krawczyk, J. Blom, R. Galvin, A. Hannigan, C. P. Dunne, A.W. Murphy, C. Mallen, Platelet-rich plasma (PRP) therapy for knee arthritis: a feasibility study in primary care, Pilot Feasibility Stud 4 (2018) 93, <https://doi.org/10.1186/s40814-018-0288-2>.
- [7] C.E. O'Hanlon, S.J. Newberry, M. Booth, S. Grant, A. Motala, M.A. Maglione, J. D. FitzGerald, P.G. Shekelle, Hyaluronic acid injection therapy for osteoarthritis of the knee: concordant efficacy and conflicting serious adverse events in two systematic reviews, Syst. Rev. 5 (1) (2016) 186, <https://doi.org/10.1186/s13643-016-0363-9>.
- [8] M.M. Cohen, R.D. Altman, R. Hollstrom, C. Hollstrom, C. Sun, B. Gipson, Safety and efficacy of intra-articular sodium hyaluronate (Hyalgan) in a randomized, double-blind study for osteoarthritis of the ankle, Foot Ankle Int. 29 (7) (2008) 657–663, <https://doi.org/10.3113/FAL.2008.0657>.
- [9] M.L. Kang, G.I. Im, Drug delivery systems for intra-articular treatment of osteoarthritis, Expert Opin. Drug Deliv. 11 (2) (2014) 269–282, <https://doi.org/10.1517/17425247.2014.867325>.
- [10] R. Barbucci, S. Lamponi, A. Borzacchiello, L. Ambrosio, M. Fini, P. Torricelli, R. Giardino, Hyaluronic acid hydrogel in the treatment of osteoarthritis, Biomaterials 23 (23) (2002) 4503–4513, [https://doi.org/10.1016/S0142-9612\(02\)00194-1](https://doi.org/10.1016/S0142-9612(02)00194-1).
- [11] J.L. Escobar Ivirico, M. Bhattacharjee, E. Kuyinu, L.S. Nair, C.T. Laurencin, Regenerative engineering for knee osteoarthritis treatment: biomaterials and cell-based technologies, Engineering 3 (1) (2017) 16–27, <https://doi.org/10.1016/j.eng.2017.01.003>.
- [12] A.L. Buchman, Side effects of corticosteroid therapy, J. Clin. Gastroenterol. 33 (4) (2001) 289–294.

- [13] N. Gerwin, C. Hops, A. Lucke, Intraarticular drug delivery in osteoarthritis, *Adv. Drug Deliv. Rev.* 58 (2) (2006) 226–242, <https://doi.org/10.1016/j.addr.2006.01.018>.
- [14] T. Kisukeda, J. Onaya, K. Yoshioka, Effect of diclofenac etalhyaluronate (SI-613) on the production of high molecular weight sodium hyaluronate in human synoviocytes, *BMC Musculoskel. Disord.* 20 (1) (2019) 201, <https://doi.org/10.1186/s12891-019-2586-0>.
- [15] A.J. Grodzinsky, Y. Wang, S. Kakar, M.S. Vrahas, C.H. Evans, Intra-articular dexamethasone to inhibit the development of post-traumatic osteoarthritis, *J. Orthop. Res.* 35 (3) (2017) 406–411, <https://doi.org/10.1002/jor.23295>.
- [16] E. Ayhan, H. Kesmezacar, I. Akgun, Intraarticular injections (corticosteroid, hyaluronic acid, platelet rich plasma) for the knee osteoarthritis, *World J. Orthoped.* 5 (3) (2014) 351–361, <https://doi.org/10.5312/wjo.v5.i3.351>.
- [17] C. Larsen, J. Ostergaard, S.W. Larsen, H. Jensen, S. Jacobsen, C. Lindegaard, P. H. Andersen, Intra-articular depot formulation principles: role in the management of postoperative pain and arthritic disorders, *J. Pharmacol. Sci.* 97 (11) (2008) 4622–4654, <https://doi.org/10.1002/jps.21346>.
- [18] H. Möllmann, P. Rohdewald, E.W. Schmidt, V. Salomon, H. Derendorf, Pharmacokinetics of triamcinolone acetonide and its phosphate ester, *Eur. J. Clin. Pharmacol.* 29 (1) (1985) 85–89, <https://doi.org/10.1007/BF00547374>.
- [19] P. Maudens, O. Jordan, E. Allemann, Recent advances in intra-articular drug delivery systems for osteoarthritis therapy, *Drug Discov. Today* 23 (10) (2018) 1761–1775, <https://doi.org/10.1016/j.drudis.2018.05.023>.
- [20] S. Turker, S. Erdogan, Y.A. Ozer, H. Bilgili, S. Deveci, Enhanced efficacy of diclofenac sodium-loaded lipogelosome formulation in intra-articular treatment of rheumatoid arthritis, *J. Drug Target.* 16 (1) (2008) 51–57, <https://doi.org/10.1080/10611860701725191>.
- [21] I. Elron-Gross, Y. Glucksam, R. Margalit, Liposomal dexamethasone-diclofenac combinations for local osteoarthritis treatment, *Int. J. Pharm.* 376 (1–2) (2009) 84–91, <https://doi.org/10.1016/j.ijpharm.2009.04.025>.
- [22] D. Guo, Q. Li, Y. Sun, J. Guo, Q. Zhao, X. Yin, H. Wei, S. Wu, H. Bi, Evaluation of controlled-release triamcinolone acetonide-loaded mPEG-PLGA nanoparticles in treating experimental autoimmune uveitis, *Nanotechnology* 30 (16) (2019) 165702, <https://doi.org/10.1088/1361-6528/aaf36>.
- [23] P. Maudens, S. Meyer, C.A. Seemayer, O. Jordan, E. Allemann, Self-assembled thermoresponsive nanostructures of hyaluronic acid conjugates for osteoarthritis therapy, *Nanoscale* 10 (4) (2018) 1845–1854, <https://doi.org/10.1039/c7nr07614b>.
- [24] N. Butoescu, C.A. Seemayer, M. Foti, O. Jordan, E. Doelker, Dexamethasone-containing PLGA superparamagnetic microparticles as carriers for the local treatment of arthritis, *Biomaterials* 30 (9) (2009) 1772–1780, <https://doi.org/10.1016/j.biomaterials.2008.12.017>.
- [25] P. Arunkumar, S. Indulekha, S. Vijayalakshmi, R. Srivastava, Synthesis, characterizations, in vitro and in vivo evaluation of Etoricoxib-delivered Poly (Caprolactone) microparticles—a potential Intra-articular drug delivery system for the treatment of Osteoarthritis, *J. Biomater. Sci. Polym. Ed.* 27 (4) (2016) 303–316, <https://doi.org/10.1080/09205063.2015.1125564>.
- [26] B. Miao, C. Song, G. Ma, Injectable thermosensitive hydrogels for intra-articular delivery of methotrexate, *J. Appl. Polym. Sci.* 122 (3) (2011) 2139–2145, <https://doi.org/10.1002/app.34332>.
- [27] L. Bedouet, F. Pascale, L. Moine, M. Wassef, S.H. Ghegediban, V.N. Nguyen, M. Bonneau, D. Labarre, A. Laurent, Intra-articular fate of degradable poly (ethylene glycol)-hydrogel microspheres as carriers for sustained drug delivery, *Int. J. Pharm.* 456 (2) (2013) 536–544, <https://doi.org/10.1016/j.ijpharm.2013.08.016>.
- [28] Z. He, B. Wang, C. Hu, J. Zhao, An overview of hydrogel-based intra-articular drug delivery for the treatment of osteoarthritis, *Colloids Surf. B Biointerfaces* 154 (2017) 33–39, <https://doi.org/10.1016/j.colsurfb.2017.03.003>.
- [29] J. Pradal, M.F. Zuluaga, P. Maudens, J.M. Waldburger, C.A. Seemayer, E. Doelker, C. Gabay, O. Jordan, E. Allemann, Intra-articular bioactivity of a p38 MAPK inhibitor and development of an extended-release system, *Eur. J. Pharm. Biopharm.* 93 (2015) 110–117, <https://doi.org/10.1016/j.ejpb.2015.03.017>.
- [30] M.L. Kang, J.-Y. Ko, J.E. Kim, G.-I. Im, THU0463, Polymer nanoparticles with thermally responsive dual release profiles for combined therapy of osteoarthritis, *Ann. Rheum. Dis.* 74 (Suppl 2) (2015) 367–368, <https://doi.org/10.1136/annrheumdis-2015-eular.6364>.
- [31] J. Kopecek, Hydrogel biomaterials: a smart future? *Biomaterials* 28 (34) (2007) 5185–5192, <https://doi.org/10.1016/j.biomaterials.2007.07.044>.
- [32] J.S. Kwon, S.M. Yoon, D.Y. Kwon, D.Y. Kim, G.Z. Tai, L.M. Jin, B. Song, B. Lee, J. H. Kim, D.K. Han, B.H. Min, M.S. Kim, Injectable in situ-forming hydrogel for cartilage tissue engineering, *J. Mater. Chem. B* 1 (26) (2013) 3314–3321, <https://doi.org/10.1039/c3tb20105h>.
- [33] C.W. Park, K.W. Ma, S.W. Jang, M. Son, M.J. Kang, Comparison of piroxicam pharmacokinetics and anti-inflammatory effect in rats after intra-articular and intramuscular administration, *Biomol. Ther. (Seoul)* 22 (3) (2014) 260–266, <https://doi.org/10.4062/biomolther.2014.037>.
- [34] K.H. Hong, Y.M. Kim, S.C. Song, Fine-tunable and injectable 3D hydrogel on-demand stem cell niche, *Adv. Sci.* 6 (17) (2019) 1900597, <https://doi.org/10.1002/advs.201900597>.
- [35] B.B. Seo, H. Choi, J.T. Koh, S.C. Song, Sustained BMP-2 delivery and injectable bone regeneration using thermosensitive polymeric nanoparticle hydrogel bearing dual interactions with BMP-2, *J. Contr. Release* 209 (2015) 67–76, <https://doi.org/10.1016/j.jconrel.2015.04.023>.
- [36] B.B. Seo, J.T. Koh, S.C. Song, Tuning physical properties and BMP-2 release rates of injectable hydrogel systems for an optimal bone regeneration effect, *Biomaterials* 122 (2017) 91–104, <https://doi.org/10.1016/j.biomaterials.2017.01.016>.
- [37] Y.-M. Kim, M.-R. Park, S.-C. Song, Injectable polyplex hydrogel for localized and long-term delivery of siRNA, *ACS Nano* 6 (7) (2012) 5757–5766, <https://doi.org/10.1021/nl300842a>.
- [38] B.B. Seo, M.R. Park, S.C. Song, Sustained release of exendin 4 using injectable and ionic-nano-complex forming polymer hydrogel system for long-term treatment of type 2 diabetes mellitus, *ACS Appl. Mater. Interfaces* 11 (17) (2019) 15201–15211, <https://doi.org/10.1021/acsami.8b19669>.
- [39] K.H. Hong, S.C. Song, 3D hydrogel stem cell niche controlled by host-guest interaction affects stem cell fate and survival rate, *Biomaterials* 218 (2019) 119338, <https://doi.org/10.1016/j.biomaterials.2019.119338>.
- [40] L.T.A. Hong, Y.M. Kim, H.H. Park, D.H. Hwang, Y. Cui, E.M. Lee, S. Yahn, J.K. Lee, S.C. Song, B.G. Kim, An injectable hydrogel enhances tissue repair after spinal cord injury by promoting extracellular matrix remodeling, *Nat. Commun.* 8 (1) (2017) 533, <https://doi.org/10.1038/s41467-017-00583-8>.
- [42] L. Bromberg, M. Temchenko, Self-assembly in aqueous solutions of poly-(ethylene oxide)-b-poly(propylene oxide)-b-poly(ethylene oxide)-bpoly(vinyl alcohol), *Langmuir* 15 (1999) 8633–8639, <https://doi.org/10.1021/la049695y>.
- [43] K. Pitarokouli, M. Sgodzai, T. Gruter, H. Bachir, J. Motte, B. Ambrosius, X. Pedreiturry, M.S. Yoon, R. Gold, Intrathecal triamcinolone acetonide exerts anti-inflammatory effects on Lewis rat experimental autoimmune neuritis and direct anti-oxidative effects on Schwann cells, *J. Neuroinflammation* 16 (1) (2019) 58, <https://doi.org/10.1186/s12974-019-1445-0>.
- [44] M.B. Goldring, M. Otero, Inflammation in osteoarthritis, *Curr. Opin. Rheumatol.* 23 (5) (2011) 471–478, <https://doi.org/10.1097/BOR.0b013e328349c2b1>.
- [45] M. Akdis, A. Aab, C. Altunbulakli, K. Azkur, J.S. Zakzuk, C.A. Akdis, Interleukins, interferons, transforming growth factor- β , and TNF- α receptors, functions, and roles in diseases, *J. Allergy Clin. Immunol.* 138 (4) (2016) 984–1010, <https://doi.org/10.1016/j.jaci.2016.06.033>.
- [46] J.-M. Zhang, J. An, Cytokines, inflammation and pain, *Int. Anesthesiol. Clin.* 45 (2) (2007) 27–37, <https://doi.org/10.1097/AIA.0b013e318034194e>.